AGU PUBLICATIONS

Geophysical Research Letters

RESEARCH LETTER
10.1002/2014GL059425

Key Points:
- Combine dense networks to construct ambient seismic field Green's functions
- The ambient seismic field contains sedimentary basin wave propagation effects
- Seismic amplification strongly depends on earthquake source location

Supporting Information:
- Text S1
- Figure S1

Correspondence to:
M. A. Denolle,
mdenolle@ucsd.edu

Citation:
Denolle, M. A., H. Miyake, S. Nakagawa, N. Hirata, and G. C. Beroza (2014), Long-period seismic amplification in the Kanto Basin from the ambient seismic field, *Geophys. Res. Lett.*, *41*, 2319–2325, doi:10.1002/2014GL059425.

Received 26 JAN 2014
Accepted 18 MAR 2014
Accepted article online 21 MAR 2014
Published online 4 APR 2014

Long-period seismic amplification in the Kanto Basin from the ambient seismic field

Marine A. Denolle[1,3], Hiroe Miyake[2], Shigeki Nakagawa[2], Naoshi Hirata[2], and Gregory C. Beroza[1]

[1]Department of Geophysics, Stanford University, Stanford, California, USA, [2]Earthquake Research Institute, University of Tokyo, Tokyo, Japan, [3]Scripps Institute of Oceanography, UCSD, San Diego, California, USA

Abstract Tokyo, like many seismically threatened cities, is situated atop a sedimentary basin that has the potential to trap and amplify seismic waves from earthquakes. We study amplification in the Kanto Basin by exploiting the information carried by the ambient seismic field. We use 375 seismic stations from the high sensitivity seismograph network across central Honshu as virtual sources and 296 seismic stations of the Metropolitan Seismic Observation network shallow borehole seismometers within the basin as receivers to map the basin response. We find a linear relationship between ground motion and basin depth at periods of 2–10 s that could be used to represent 3-D basin effects in ground motion prediction equations. We also find that the strength of basin seismic amplification depends strongly on the direction of illumination by seismic waves.

1. Introduction

Sedimentary basins surrounded by stiffer bedrock have a strong effect on earthquake ground motion because they trap and amplify seismic waves [*Anderson et al.*, 1986]. Basin effects can overwhelm the amplitude decay with distance from the earthquake source. The most dramatic example of strong seismic amplification distant from the source is the *M* 8.0 Michoacán, 1985, earthquake, which devastated Mexico City despite the rupture being located at a distance of about 300 km. This earthquake led the seismological community to pay closer attention to wave propagation effects in soft sediments [*Bard et al.*, 1988; *Aki*, 1993].

The most common approach to ground motion prediction uses parametric ground motion prediction equations (GMPEs) to relate shaking intensity to source, distance, and site characteristics. GMPEs do not commonly incorporate three-dimensional wave propagation effects and are limited by a lack of data for large earthquakes at short distances. Physics-based simulations can compensate for this by modeling seismic wave propagation in complex crustal velocity structure [*Olsen et al.*, 2006; *Graves et al.*, 2011; *Day et al.*, 2012]. These simulations show the strong influence of basin structure in amplifying ground motion. *Day et al.* [2008] proposed adding a term to GMPEs to represent basin effects, and *Campbell and Bozorgnia* [2013] used data from California and Japan to constrain this term. Given the limitations of available strong ground motion data, both GMPEs and simulations would benefit from additional observations.

The combination of high seismic activity, state-of-the-art dense seismic networks, and complex crustal structure in Japan provides the ideal opportunity to improve the understanding of basin effects. *Miyake and Koketsu* [2005] used earthquakes off the Kii Peninsula to observe seismic excitation of the Osaka, Nagoya, and Kanto Basins. In each case they found relatively long-period (5–10 s) resonances, which are controlled by the shape and wave speed of the basins. Seismic amplification was also observed in the Kanto Basin during the *M* 6.6 Chuetsu, 2004, earthquake [*Furumura and Hayakawa*, 2007].

The Kanto sedimentary basin, which underlies Tokyo, consists of sediments with *S* wave velocities V_S as low as 500 m/s [*Yamanaka and Yamada*, 2002; *Tanaka et al.*, 2005] and basement as deep as 4 km underneath Chiba prefecture [*Koketsu et al.*, 2009]. The concave structure of the basin combined with the low wave speed of the sediments leads to a resonance period of approximately 7 s [*Furumura and Hayakawa*, 2007]. Figure 1 shows depth contours of the V_S = 3.2 km/s isosurface, which is used by *Koketsu et al.* [2009] as a measure of basin depth. *Furumura and Hayakawa* [2007] used a combination of observations and simulation of the 2004 Chuetsu earthquake to demonstrate the presence of a seismic waveguide near the Gunma Pass that funnels seismic waves from the Niigata Basin into the Kanto Basin. Central Honshu has a large number of historically active faults (Figure 1) [*Advanced Industrial Science and Technology (AIST)*, 2012]

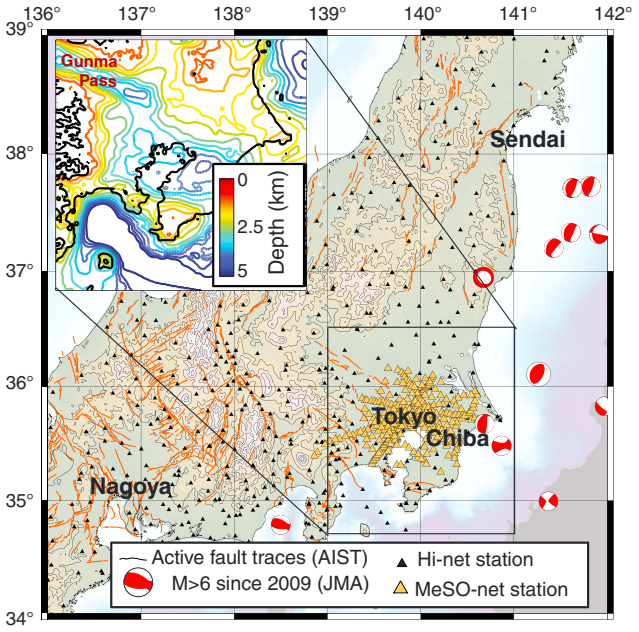

Figure 1. Kanto Basin with basement depth (upper left inset) [*Koketsu et al.*, 2009], MeSO-net stations (solid orange triangles), Hi-net stations (solid dark triangles), *M* 6 earthquakes between 2009 and 2013 (Japan Meteorological Agency (JMA) location, National Research Institute for the Earth Science and Disaster Prevention moment tensor solutions), and active fault traces (solid brown curves) from the Research Information Database DB095 [*Advanced Industrial Science and Technology (AIST)*, 2012].

that could direct seismic waves into this waveguide in future earthquakes. Waveguides in other settings are known to enhance seismic amplification by channeling waves into sedimentary basins [*Olsen et al.*, 2006; *Day et al.*, 2012; *Denolle et al.*, 2014].

The dense Metropolitan Seismic Observation network (MeSO-net) [*Sakai and Hirata*, 2009; *Kasahara et al.*, 2009] was deployed with the primary scientific goal of characterizing the deep structure and tectonics of the plate boundaries under Tokyo. The 296 shallow borehole instruments in urban Tokyo (Figure 1) also provide an exceptional opportunity to study basin effects. *Tsuno et al.* [2012] used earthquakes of M_{JMA} (magnitude from the Japan Meteorological Agency) greater than 6 that occurred since 2009 to measure seismic amplification and basin resonance.

In this study, we use the ambient seismic field to explore basin response. We treat stations outside the basin as virtual sources and stations inside the basin as receivers. We estimate the vertical-to-vertical impulse responses from all sources (Hi-net stations, Figure 1) [*Okada et al.*, 2004; *Obara et al.*, 2005] in central Honshu to all receivers (MeSO-net stations, Figure 1) [*Sakai and Hirata*, 2009] in the Kanto Basin. Although predictions of horizontal strong ground motion is of greater interest for seismic hazard characterization, we focus in this paper on the vertical response for two reasons. First, the vertical component data have a higher signal-to-noise ratio and yield a more stable amplitude response. Second, the basin response includes both Rayleigh and Love waves with conversions at the basin boundary, and we focus this study on the basin resonance of Rayleigh waves.

We calculate the averaged relative peak amplitude of the impulse responses in the period band of interest (2–10 s). Our results support previous correlations between basin resonance and velocity structure [*Miyake and Koketsu*, 2005]. We also find an increase in amplitude of long-period vertical ground motion with sediment thickness, and we construct a simple linear relationship that captures both seismic amplification of long-period ground motion with the basin depth and the natural resonance of the basin at 5–6 s. Finally, we find that the excitation of the basin resonance strongly depends on the source location.

2. Ambient Seismic Field Green's Functions

The surface wave fundamental mode typically dominates the correlation functions constructed from the ambient seismic field [*Shapiro and Campillo*, 2004; *Sabra et al.*, 2005]. We construct ambient seismic field Green's functions [*Prieto and Beroza*, 2008; *Seats et al.*, 2011; *Denolle et al.*, 2013] using

$$\widehat{G}_{AB}(\omega) = \left\langle \frac{\hat{v}_i(\mathbf{x}_B,\omega)\hat{v}_j^*(\mathbf{x}_A,\omega)}{\{|\hat{v}_j(\mathbf{x}_A,\omega)|\}^2} \right\rangle \quad , \tag{1}$$

where A is the virtual source and B is the receiver, $\hat{v}_i(\mathbf{x}_A,\omega)$ and $\hat{v}_j(\mathbf{x}_B,\omega)$ are their respective ambient field vertical velocity spectra. The operator $\langle\ \ \rangle$ denotes stacking over time windows, and $\{\ \ \}$ denotes smoothing over the virtual source spectrum (10-point running average) to ensure stability in the deconvolution.

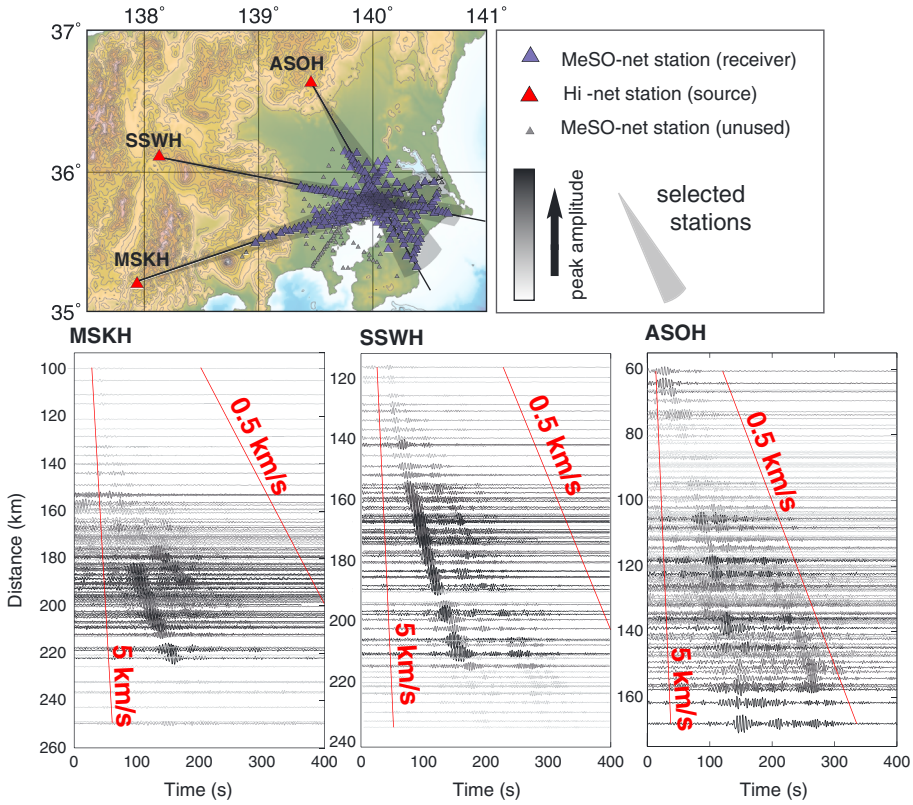

Figure 2. Seismic amplification in the Kanto Basin view from three virtual sources (ASOH, SSWH, and MSKH) along lines of seismometers and across the basin. Gray-scale waveforms filtered 3–10 s, colored according to peak amplitude for clarity, and corrected for the surface wave geometrical decay $\sqrt{r}$. Amplification occurs in the central part of the Kanto Basin.

We use 1 h time series from continuous recordings between January and June, 2013, and detect coherent signal from 2 to 10 s for distances up to 300 km. We measure the peak amplitude of the (2–10 s) band-pass filtered Green's function on either the causal (positive lag) or anticausal (negative lag) side, depending on which side has greater signal-to-noise ratio, and correct for the surface-wave geometrical spreading of $1/\sqrt{r}$, where r is the distance between seismic stations.

The Green's functions from virtual sources outside the basin to receivers inside the basin are characterized by large amplitudes and pronounced dispersion (Figure 2). We anticipate such effects from the strong interaction between seismic waves and soft sediments in the shallow layers [*Boore et al.*, 1971; *Wald and Graves*, 1998] that have particularly low wave speed (less than 500 m/s). Despite a nonuniform distribution of the microseismic energy, predominantly from the Pacific Ocean, our measurements do not exhibit strong directional variation of amplitude with azimuth due to directionality of the microseism (see Figure S1a in the supporting information). The distribution of stations with azimuth is highly nonuniform (see Figure S1b in the supporting information), and we account for this using an azimuthally smooth weighting function to approximate a uniform seismic illumination of the Kanto Basin.

Unlike conventional estimates of ground motion that combine source characteristics and wave propagation effects, such as peak ground velocity or peak ground acceleration, we construct nondimensional Green's functions (equation (1)) that preserves relative amplitude information. We measure basin response using the relative peak values, which we denote as peak ground motion (PGM). PGM reflects the seismic amplification due solely to linear wave propagation effects. Our estimate of the seismic amplification is relative to a representative value of ground motion at a given frequency (equation (3)).

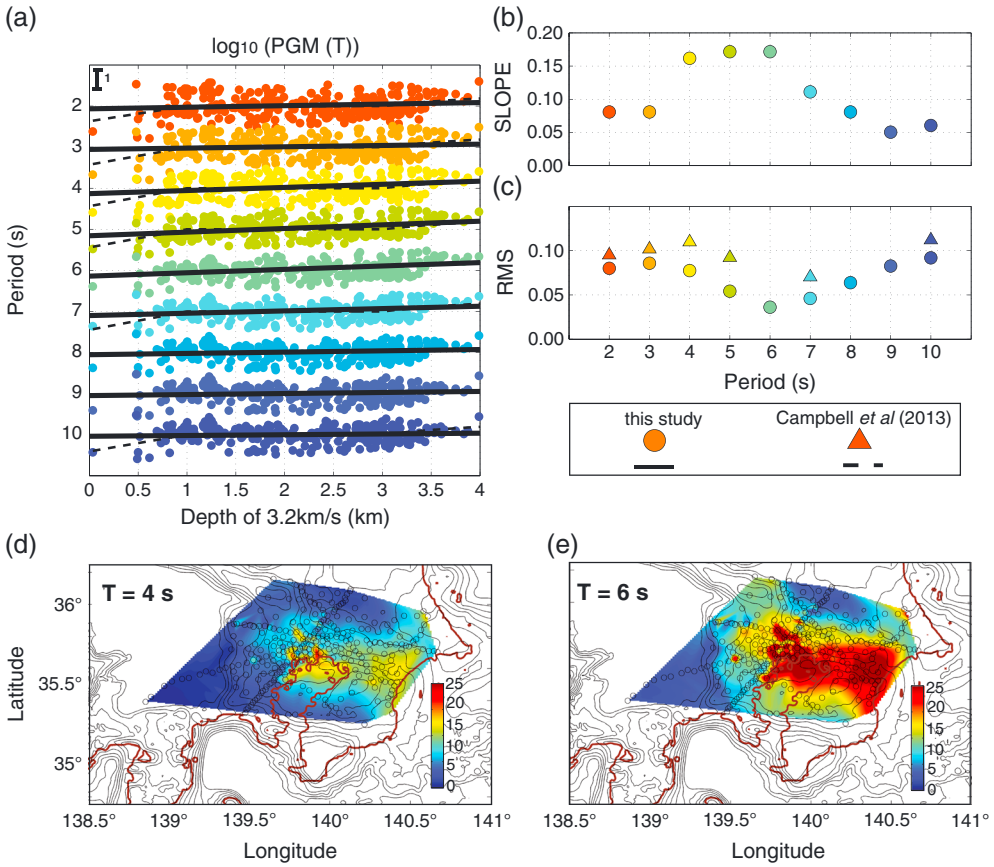

Figure 3. For clarity, we color the observation at different periods accordingly. (a) Base-10 logarithm of the PGM amplitude for different periods T as a function of basin depth (V_S = 3.2 km/s isosurface); dashed lines are the best fit basin term (equation (1)); solid lines are the linear fit of equation (2). (b) Best fit slope of equation (2) with period $a(T)$. (c) Root-mean-square residuals of the fit to equation (1) (filled triangles) and to equation (2) (filled circles) and the observations. (d–e) Amplification factor map between lowest-to-highest peak ground motion at periods of 4 and 6 s. Brown solid lines are coastlines. Black solid contours are 500 m spaced for the V_S = 3.2 km/s isosurface depth. Color scale shows the amplification factor.

3. Ground Motion Prediction From Basin Depth

A simple way to incorporate the effect of basin sediments on ground motion is to correlate the observed peak amplitudes with the basin depth. *Day et al.* [2008] used ground motion simulations to develop a spectral response model as a function of basin depth to characterize basin effects in the GMPEs. We narrow-pass filter the data at periods ranging from 2 and 10 s. We use the parametric form of this function, which accounts for basin response from *Campbell and Bozorgnia* [2013], and test it against our observations of vertical peak ground motion (Figure 3). We predict the contribution of the parametric function to each period of the peak ground motion (PGM):

$$\log_{10}(\mathrm{PGM}(T)) = \begin{cases} (c_{14}(T) + c_{15}(T))(Z_{2.5} - 1) & ; \quad Z_{2.5} \le 1 \\ 0 & ; \quad 1 < Z_{2.5} \le 3 \\ c_{16}(T)k_3(T)e^{-0.75}\left[1 - e^{-0.25(Z_{2.5}-3)}\right] & ; \quad Z_{2.5} \ge 3 \end{cases}, \tag{2}$$

where the coefficients c_{14}, c_{15}, c_{16}, and k_3 depend on the period T and $Z_{2.5}$ is the basin depth, which we take as the V_S = 3.2 km/s isosurface depth [*Koketsu et al.*, 2009]. *Campbell and Bozorgnia* [2013] find the GMPE parameters by fitting this functional form to recorded horizontal ground motion intensities. The GMPEs fit well our observations of vertical ground motion, particularly around the basin resonance periods of

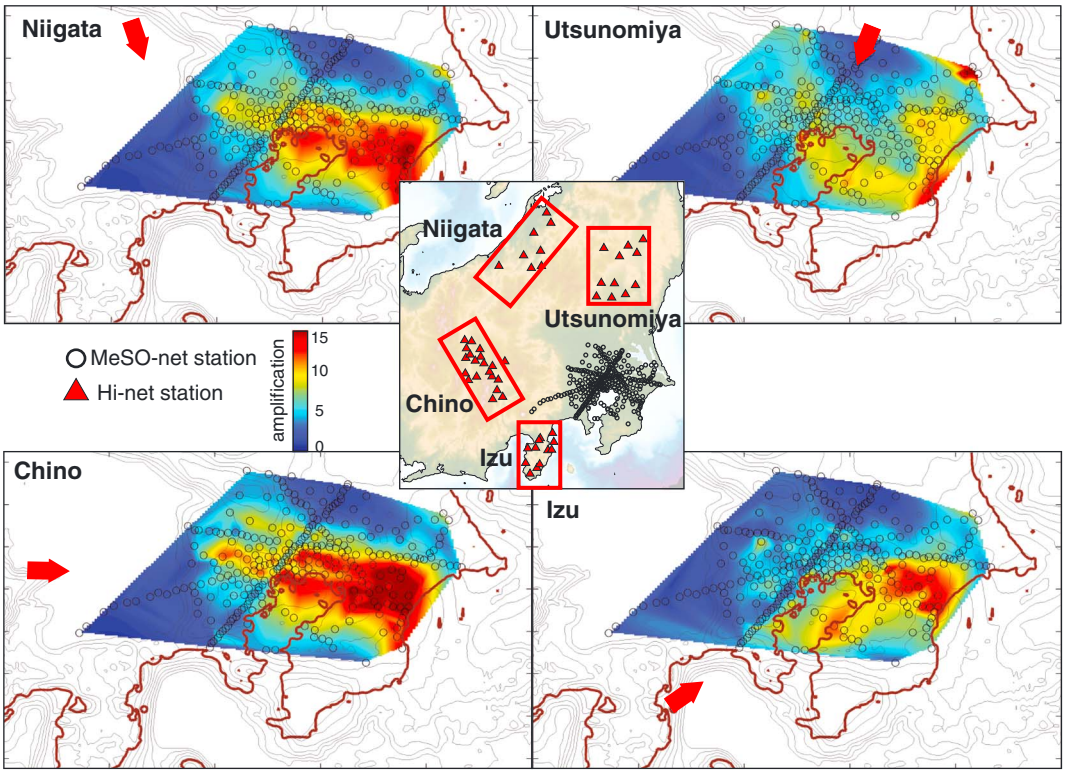

Figure 4. Amplification maps similar to Figures 3d and 3e with coast lines (brown lines), basement contours 500 m spaced (black lines), at 6 s period, and for targeted virtual source regions. For each MeSO-net station (black circles), we average the amplitudes over the virtual sources (red triangles) within the red rectangle.

5 and 7 s. Our measurements suggest a simple linear expression to represent the variation of ground motion with basin depth as a function of only two parameters:

$$\log_{10}(\mathrm{PGM}(T)) = a(T)Z_{3.2} + b(T). \quad (3)$$

where the basin depth is $Z_{3.2}$. We show the best fit slope $a(T)$ in Figure 3b. We find a variable scaling that has the strongest dependence on basin depth at 5–6 s, periods at which we also minimize the root-mean-square residual. This scaling relation allows us to estimate a representative value for the peak ground motion amplitudes at a given frequency $b(T)$ (equation (3)) that varies due to the spectrum of the Green's functions. We estimate the seismic amplification factor from normalizing PGM(T) by $b(T)$.

Our results suggest that seismic amplification increases, to first order, proportionally with basin depth, and most strongly at the resonance period. We see that most of the amplification follows spatially the structure of the basin, with shorter periods amplified near shallow parts of the basin (Figure 3d) and longer periods amplified near deeper parts (Figure 3e). Simulations and observations of horizontal ground motion yield a resonance at longer period (7–10 s) with a peak amplification factor ranging between 10 and 16 for seismic waves coming from the southwest [*Miyake and Koketsu*, 2005] and from the northwest [*Furumura and Hayakawa*, 2007] and of short period (5–6 s) for seismic waves coming from the north and east [*Tsuno et al.*, 2012]. Our amplification measurements are based on the vertical component of the Rayleigh waves which directly correlates with the horizontal component due to the elliptical particle motion of the Rayleigh waves. The extensive station coverage allows us to examine the excitation of the basin from all azimuths, though there are relatively fewer stations to the south and west.

4. Seismic Amplification in the Kanto Basin

Based on the 375 virtual sources, we find a positive correlation between seismic amplification and sedimentary basin depth. Ground motion is amplified up to 25 times for the center of the basin relative to its surroundings (Figures 3d and 3e). We expect nonlinearity to moderate such amplification during strong

ground motion, and it is likely to reduce this amplification factor [*Roten et al.*, 2012]. The northern end of the seismic network is situated atop deep half-grabens at the Gunma Pass [*Takahashi et al.*, 2004] that may channel seismic waves from the Niigata Basin into the Kanto Basin [*Furumura and Hayakawa*, 2007], and we see the resonance of the waveguide at 6 s period on the amplification map (Figure 3e).

The amplification pattern varies significantly with the direction of incoming seismic waves. Note that we use the maximum (causal or anticausal) Green's function amplitude in each case, and for this measure the observed azimuthal distribution (Figure S1b) is not affected by directionality of the ambient seismic field. This suggests that the variations instead arise from the propagation effects from the virtual source to the receivers. Given four distinct source regions, we show in Figure 4 the amplification map due to wave propagation effects.

In the first source region, the Niigata Basin, the sources trigger strong excitation in the waveguide from the Gunma Pass to the Kanto Basin. This observation supports the hypothesis and modeling results of *Furumura and Hayakawa* [2007] that sources in the Niigata region will strongly excite resonance of the Kanto Basin. The amplification from the second source region, in Tochigi, is not particularly strong in the Kanto Basin. This is consistent with the weak basin amplification observed for the 2011 Fukushima-Hamadori normal-faulting earthquake [*Tsuno et al.*, 2012] and the 2005 Miyagi-oki earthquake.

The amplification from sources in the Suwa-Kofu areas is striking as we do not see interaction with the waveguide, yet it shows strong amplitudes for seismic waves near the western basin edge. This suggests the potential importance of basin edge effects on ground motion [*Kawase*, 1996; *Pitarka et al.*, 1998; *Graves et al.*, 1998]. Finally, we predict that sources in the Izu Peninsula should strongly excite long-period ground motion in Chiba prefecture, where *Koketsu and Kikuchi* [2000] proposed that the refraction of seismic waves along the basin edge increases ground motion in Tokyo.

5. Conclusions

We constructed the Earth's impulse response for vertical-to-vertical components of the Green tensor for 375 virtual sources at Hi-net borehole instruments across central Honshu, to 296 receivers at the MeSO-net boreholes seismometers in the Kanto Basin. The surface-to-surface responses extracted from the ambient seismic field are strongly affected by the presence the sedimentary basin and show strong seismic amplification at periods of interest for long-period ground motion prediction. Our results are consistent with basin effects observed during the *M* 6.6 Chuetsu, 2004, earthquake and in ground motion simulations [*Furumura and Hayakawa*, 2007].

With the exceptional data coverage for both the virtual sources and the receivers, we build seismic amplification maps from the averaged peak amplitude measurements of the impulse responses. Strong amplification occurs within the basin and peaks at periods 5–6 s where the basin is the deepest. We find a simple linear relation between peak ground motion and basin depth. This relation provides a simple and useful functional form that could be used for the GMPEs to approximate complex three- dimensional effects. We anticipate the interaction with the waveguide to the northwest, and the basin edge to the west, will significantly affect the ground motion within the Kanto Basin. In the future, estimates of amplification using the horizontal components may reveal basin edge effects [*Graves et al.*, 1998]. We limited our study to the Rayleigh-wave basin response. Preliminary results for the horizontal components reveal important coupling between Rayleigh and Love waves. Understanding the contributions from Rayleigh and Love waves in ground motion will require a careful analysis of the full 3-D wave field excitation and coupling using all nine components of the Green's function.

This study is an example of the extraordinary potential of dense seismic networks to characterize seismic hazards in an urban environment. Our results highlight the power of using the ambient seismic field to investigate basin amplification for future large earthquakes.

Acknowledgments

We used earthquake catalogs of the JMA, the fault locations from AIST. This work was partially supported by the NSF grant EAR-0943885, by the NSF grant EAR-0949443, by the Special Project for Reducing Vulnerability for Urban Mega Earthquake Disasters from the Ministry of Education, Culture, Sports, Science, and Technology of Japan and was supported by the SAVI supplement to NSF cooperative agreement EAR-1033462. SCEC is funded by NSF cooperative agreement EAR-0529922 and USGS cooperative agreement 07HQAG0008. The SCEC contribution for this paper is 1836.

The Editor thanks an anonymous reviewer for his/her assistance in evaluating this paper.

References

Advanced Industrial Science and Technology (AIST) (2012), Active fault database of Japan, February 28, 2012 version, research information database DB095, National Institute of Advanced Industrial Science and Technology (AIST), Japan.

Aki, K. (1993), Local site effects on weak and strong ground motion, *Tectonophysics*, *218*, 93–111, doi:10.1016/0040-1951(93)90262-I.

Anderson, J. G., P. Bodon, J. N. Brune, J. Prince, S. K. Sing, R. Quaas, and M. Onate (1986), Strong ground motion from the Michoacan, Mexico, earthquake, *Science*, *233*, 1043–1049.

Bard, P.-Y., M. Campillo, F. J. Chávez-Garcia, and F. J. Sánchez-Sesma (1988), The Mexico earthquake of September 19, 1985—A theoretical investigation of large- and small-scale amplification effects in the Mexico City Valley, *Earthquake Spectra*, *4*(3), 609–633.

Boore, D. M., K. L. Larner, and K. Aki (1971), Comparison of two independent methods for the solution of wave-scattering problems: Response of a sedimentary basin to vertically incident SH waves, *J. Geophys. Res.*, *76*(2), 558–569.

Campbell, K. W., and Y. Bozorgnia (2013), NGA-West2 Campbell-Bozorgnia ground motion model for the horizontal components of PGA, PGV, and 5%-damped elastic pseudo-acceleration response spectra for periods ranging from 0.01 to 10 sec, *PEER Report 2013/06*.

Day, S. M., R. Graves, J. Bielak, D. Dreger, S. Larsen, K. B. Olsen, A. Pitarka, and L. Ramirez-Guzman (2008), Model for basin effects on long-period response spectra in Southern California, *Earthquake Spectra*, *24*(1), 257–277.

Day, S. M., D. Roten, and K. B. Olsen (2012), Adjoint analysis of the source and path sensitivities of basin-guided waves, *Geophys. J. Int.*, *189*, 1103–1124.

Denolle, M. A., E. M. Dunham, G. A. Prieto, and G. C. Beroza (2013), Ground motion prediction of realistic earthquake sources using the ambient seismic field, *J. Geophys. Res. Solid Earth*, *118*, 2102–2118, doi:10.1029/2012JB009603.

Denolle, M. A., E. M. Dunham, G. A. Prieto, and G. C. Beroza (2014), Strong ground motion prediction using virtual earthquakes, *Science*, *343*, 399–403, doi:10.1126/science.1245678.

Furumura, T., and T. Hayakawa (2007), Anomalous propagation of long-period ground motions recorded in Tokyo during the 23 October 2004 Mw 6.6 Niigata-ken Chuetsu, Japan, Earthquake, *Bull. Seismol. Soc. Am.*, *97*(3), 863–880.

Graves, R., A. Pitarka, and P. G. Somerville (1998), Ground-motion amplification in the Santa Monica area: Effects of shallow basin-edge structure, *Bull. Seismol. Soc. Am.*, *88*(5), 1224–242.

Graves, R., et al. (2011), Cybershake: A physics-based seismic hazard model for Southern California, *Pure Appl. Geophys.*, *168*(3-4), 367–381.

Kasahara, K., S. Sakai, Y. Morita, N. Hirata, N. Tsuruoka, S. Nakagawa, K. Nanjo, and K. Obara (2009), Development of the Metropolitan Seismic Observation Network (MeSO-net) for detection of mega-thurst beneath Tokyo metropolitan area, *Bull. Earthquake Res. Inst. Univ. Tokyo*, *84*, 71–88.

Kawase, H. (1996), The cause of the damage belt in Kobe, the "basin edge effect", constructive interference of the direct S-wave with the basin-induced diffracted/Rayleigh waves, *Seismol. Res. Lett.*, *67*(5), 25–34.

Koketsu, K., and M. Kikuchi (2000), Propagation of seismic ground motion in the Kanto Basin, Japan, *Science*, *288*(5469), 1237–1239.

Koketsu, K., H. Miyake, Afnimar, and Y. Tanaka (2009), A proposal for a standard procedure of modeling 3-D velocity structures and its application to the Tokyo metropolitan area, Japan, *Tectonophysics*, *472*, 290–300.

Miyake, H., and K. Koketsu (2005), Long-period ground motions from a large offshore earthquake: The case of teh 2004 off the Kii peninsula earthquake, Japan, *Earth Planets Space*, *57*, 203–207.

Obara, K., K. Kasahara, S. Hori, and Y. Okada (2005), A densely distributed high-sensitivity seismograph network in Japan: Hi-net by National Research Institute for Earth Science and Disaster Prevention, *Rev. Sci. Instrum.*, *76*, 021301.

Okada, Y., K. Kasahara, K. Obara, S. Sekuguchi, H. Fujiwara, and A. Yamamoto (2004), Recent progress of seismic observation networks in Japan -Hi-net, F-net, K-NET and KiK-net, *Earth Planets and Space*, *56*, 15–28.

Olsen, K., S. M. Day, J. Minster, Y. Cui, A. Chourasia, M. Faerman, R. Moore, P. Maechling, and T. Jordan (2006), Strong shaking in Los Angeles expected from southern San Andreas earthquakes, *Geophys. Res. Lett.*, *33*, L07305, doi:10.1029/2005GL025472.

Pitarka, A., K. Irikura, T. Iwata, and H. Sekiguchi (1998), Three-dimensional simulation of the near-fault ground motion for the 1995 Hyogo-ken Nanbu (Kobe), Japan, Earthquake, *Bull. Seismol. Soc. Am.*, *88*(2), 428–440.

Prieto, G. A., and G. C. Beroza (2008), Earthquake ground motion prediction using the ambient seismic field, *Geophys. Res. Lett.*, *35*, L14304, doi:10.1029/2008GL034428.

Roten, D., K. B. Olsen, and J. C. Pechmann (2012), 3D simulations of M 7 earthquakes on the Wasatch Fault Utah, Part II: Broadband (0-10 Hz) ground motions and nonlinear soil behavior, *Bull. Seismol. Soc. Am.*, *102*(5), 2008–2030.

Sabra, K. G., P. Gerstoft, P. Roux, W. A. Kuperman, and M. C. Fehler (2005), Extracting time-domain Green's function estimates from ambient seismic noise, *Geophys. Res. Lett.*, *32*, L03310, doi:10.1029/2004GL021862.

Sakai, S., and N. Hirata (2009), Distribution of the Metropolitan Seismic Observation network, *Bull. Earthquake Res. Inst. Univ. Tokyo*, *84*, 57–69.

Seats, K. J., J. F. Lawrence, and G. A. Prieto (2011), Improved ambient noise correlation functions using Welch's methods, *Geophys. J. Int.*, *188*, 513–523, doi:10.1111/j.1365-246X.2011.05263.x.

Shapiro, N. M., and M. Campillo (2004), Emergence of broadband Rayleigh waves from correlations of the ambient seismic noise, *Geophys. Res. Lett.*, *31*, L07614, doi:10.1029/2004GL019491.

Takahashi, M., Y. Yanagisawa, H. Hayashi, K. Kasahara, T. Ikawa, T. Kawanaka, and S. Suda (2004), Miocene subsurface half-grabens in the Kanto Plain, central Japan, *International Workshop on Strong Ground Motion Prediction and Earthquake Tectonics in Urban Areas*, 65–74, Earthquake Research Institute, Univ. of Tokyo, Japan.

Tanaka, Y., K. Koketsu, H. Miyake, T. Furumura, H. Sato, N. Hirata, H. Suzuki, and T. Masuda (2005), Integrated modeling of 3D velocity structure beneath the Tokyo metropolitan area, *Eos Trans. AGU*, *86*(52), Abstract S21A–0200.

Tsuno, S., H. Yamanaka, S. Midorikawa, S. Yamamoto, H. Miura, S. Sakai, N. Hirata, K. Kasahara, H. Kimura, and T. Aketagawa (2012), Characteristics of long-period ground motions in the Tokyo metropolitan area and its vicinity, by recording data of the 2011 off the Pacific Coast of Tohoku Earthquake (Mw 9.0) and the aftershocks, *J. Jpn. Assoc. Earthquake Eng.*, *12*(5), 102–116.

Wald, D. J., and R. Graves (1998), The seismic response of the Los Angeles Basin, California, *Bull. Seismol. Soc. Am.*, *88*(2), 337–356.

Yamanaka, H., and N. Yamada (2002), Estimation of 3D S-wave velocity model of deep sedimentary layers in Kanto basin, Japan, using microtremor array measurements, *Butsuri-Tansa (Geophysical exploration)*, *55*, 53–66.